Following a CME from the Sun to the inner heliosphere: The 2013 August 19 event

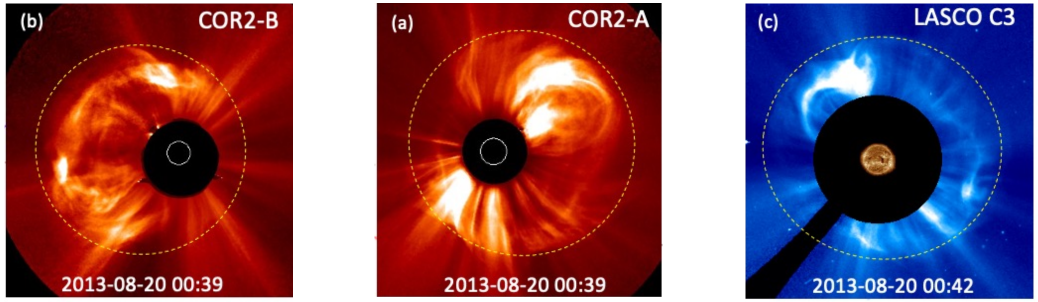

Evidence of a complex structure within the 2013 August 19 coronal mass ejection

Radial and longitudinal evolution in the inner heliosphere

Rodríguez-García et al. 2022 (A&A)

L. Rodríguez-García[1], T. Nieves-Chinchilla[2], R. Gómez-Herrero[1], I. Zouganelis[3], A. Vourlidas[4], L. Balmaceda[2,5], M. Dumbović[6], L. K. Jian[2], L. Mays[2], F. Carcaboso[1], L. F. G. dos Santos[7], and J. Rodríguez-Pacheco[1]

Laura Rodríguez García
Postdoctoral researcher at Universidad de Alcalá (Madrid, Spain)
Solar Orbiter EPD instrument team member
SERPENTINE project member

Financial support by the Spanish Ministerio de Ciencia, Innovación y Universidades FEDER/MCIU/AEI Projects ESP2017-88436-R and PID2019-104863RB I00/AEI/10.13039/501100011033

The unusual solar energetic particle event on 2013 August 19

https://www.aanda.org/articles/aa/abs/2021/09/aa39960-20/aa39960-20.html

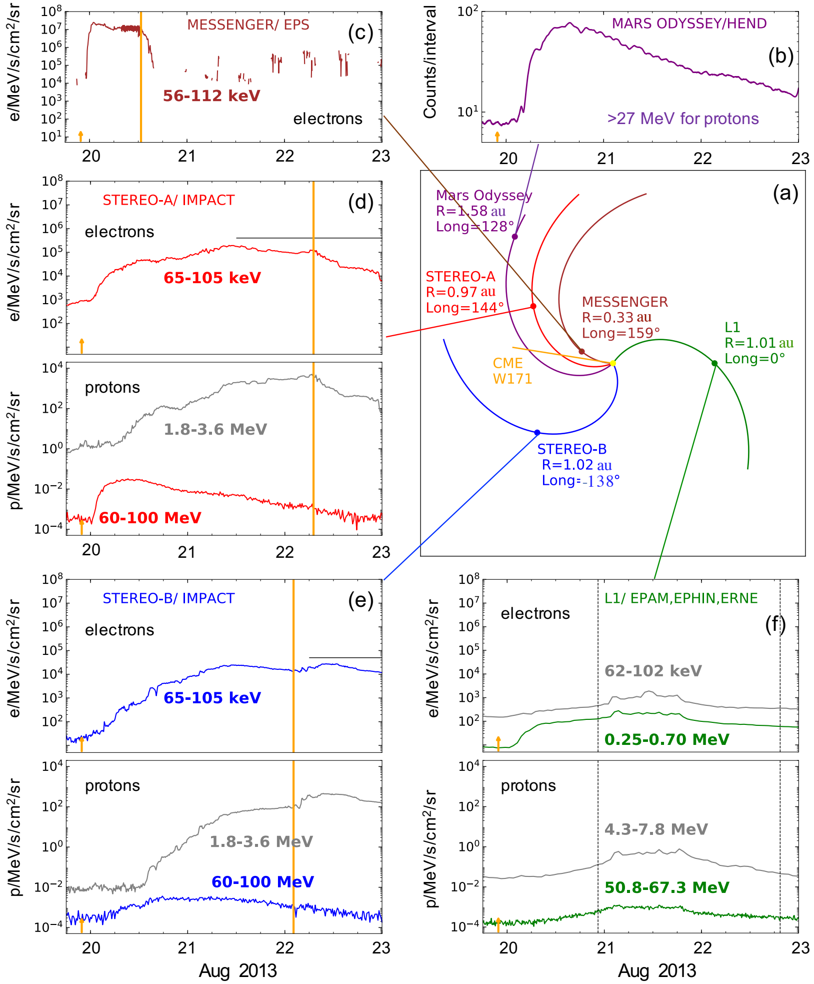

edp sciences

Astronomy & Astrophysics | All volumes | For authors

Home ▸ All issues ▸ Volume 653 (September 2021) ▸ A&A, 653 (2021) A137 ▸ Abstract

Issue	A&A Volume 653, September 2021
Article Number	A137
Number of page(s)	22
Section	The Sun and the Heliosphere
DOI	https://doi.org/10.1051/0004-6361/202039960
Published online	24 September 2021

A&A 653, A137 (2021)

The unusual widespread solar energetic particle event on 2013 August 19

Solar origin and particle longitudinal distribution*

L. Rodríguez-García[1], R. Gómez-Herrero[1], I. Zouganelis[2], L. Balmaceda[3,4], T. Nieves-Chinchilla[3], N. Dresing[5,6], M. Dumbović[7], N. V. Nitta[8], F. Carcaboso[1], L. F. G. dos Santos[9], L. K. Jian[3], L. Mays[3], D. Williams[2] and J. Rodríguez-Pacheco[1]

Received: 22 November 2020 | **Accepted:** 22 June 2021

Abstract

Context. Late on 2013 August 19, STEREO-A, STEREO-B, MESSENGER, Mars Odyssey, and the L1 spacecraft, spanning a longitudinal range of 222° in the ecliptic plane, observed an energetic particle flux increase. The widespread solar energetic particle (SEP) event was associated with a coronal mass ejection (CME) that came from a region located near the far-side central meridian from Earth's perspective. The

Financial support by the Spanish Ministerio de Ciencia, Innovación y Universidades FEDER/MCIU/AEI Projects ESP2017-88436-R and PID2019-104863RB I00/AEI/10.13039/501100011033

ICME (Interplanetary coronal Mass ejection)

IP shock: Interplanetary shock
MO: Magnetic Obstacle
MC: Magnetic Cloud

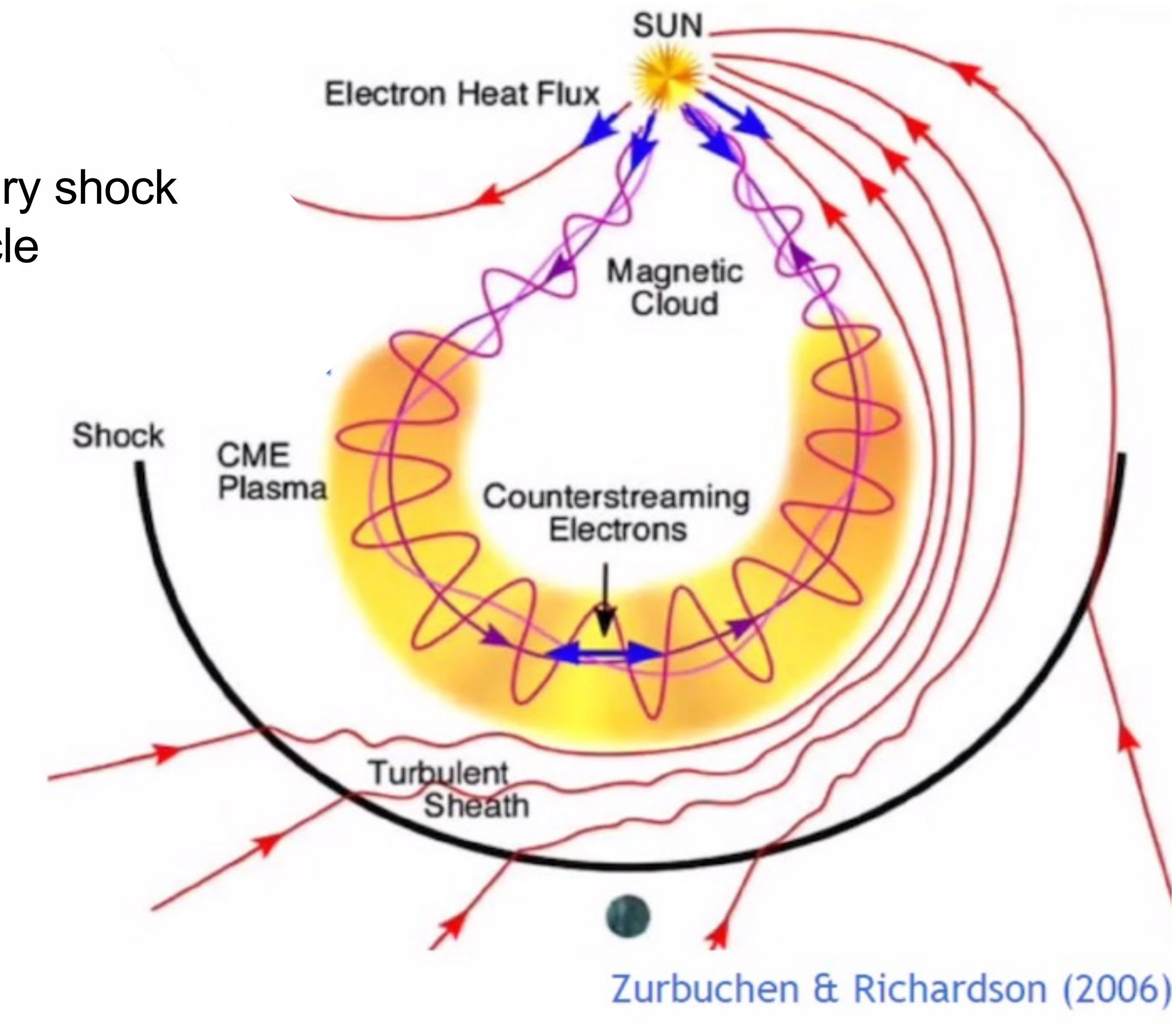

Financial support by the Spanish Ministerio de Ciencia, Innovación y Universidades FEDER/MCIU/AEI Projects ESP2017-88436-R and PID2019-104863RB I00/AEI/10.13039/501100011033

Magnetic cloud type

Kilpua et al. 2011: “Multipoint ICME encounters: Pre-STEREO and STEREO observations”

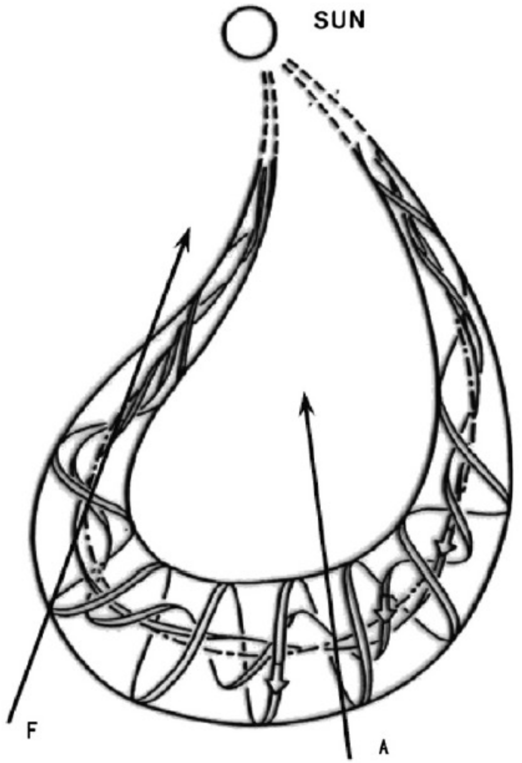

Fig. 1. Flux rope curved along the Parker spiral (Marubashi and Lepping, 2007).

Kilpua et al. 2011

Magnetic Cloud Type	SEN	SWN	NES	NWS
Leading Field	South (-Bz)	South (-Bz)	North (+Bz)	North (+Bz)
Axial Field	East (+By)	West (-By)	East (+By)	West (-By)
Trailing Field	North (+Bz)	North (+Bz)	South (-Bz)	South (-Bz)
Helicity	LH	RH	RH	LH

Magnetic Cloud Type	WNE	ESW	ENW	WSE
Leading Field	West (-By)	East (+By)	East (+By)	West (-By)
Axial Field	North (+Bz)	South (-Bz)	North (+Bz)	South (-Bz)
Trailing Field	East (+By)	West (-By)	West (-By)	East (+By)
Helicity	RH	RH	LH	LH

Fig. 2. The flux rope categories for bipolar ICMEs (top) and for unipolar ICMEs (bottom). The figures are from the Mulligan et al. (1998) work.

Kilpua et al. 2011

Financial support by the Spanish Ministerio de Ciencia, Innovación y Universidades FEDER/MCIU/AEI Projects ESP2017-88436-R and PID2019-104863RB I00/AEI/10.13039/501100011033

Coronal mass ejection on 2013 August 19

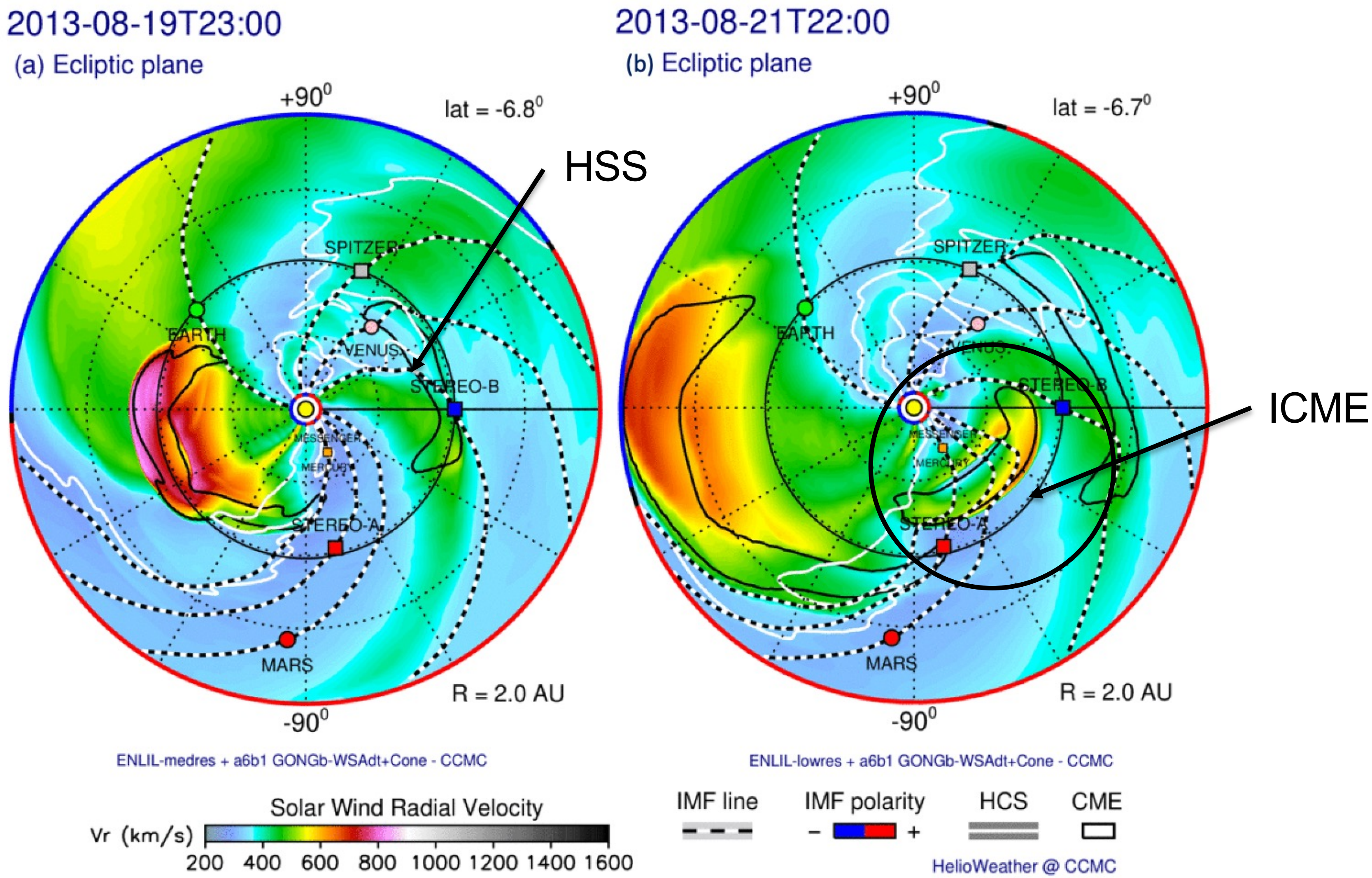

https://ccmc.gsfc.nasa.gov/database_SH/Laura_Rodriguez-Garcia_093020_SH_2.php

Financial support by the Spanish Ministerio de Ciencia, Innovación y Universidades FEDER/MCIU/AEI Projects ESP2017-88436-R and PID2019-104863RB I00/AEI/10.13039/501100011033

Coronal mass ejection on 2013 August 19

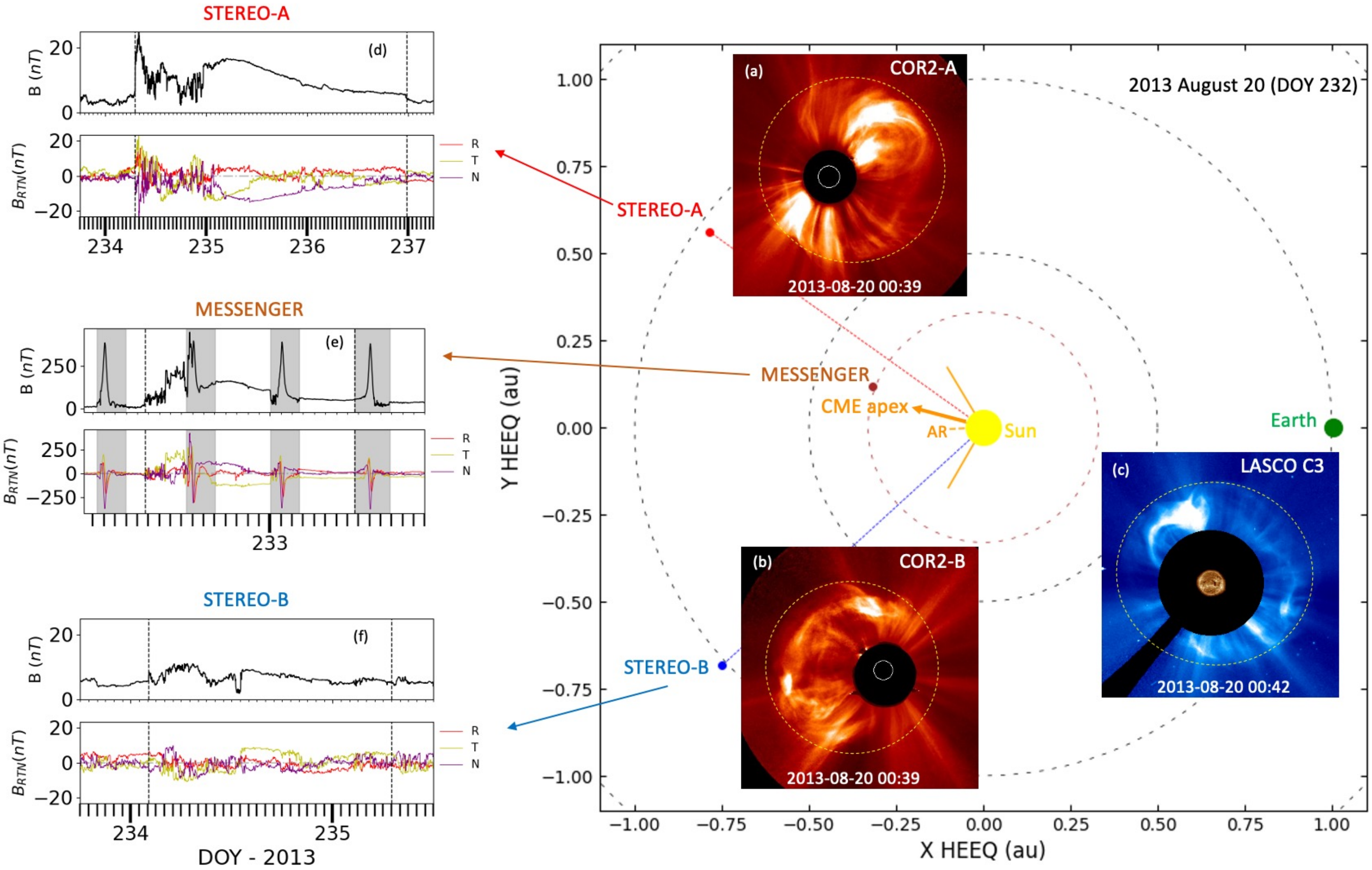

Financial support by the Spanish Ministerio de Ciencia, Innovación y Universidades FEDER/MCIU/AEI Projects ESP2017-88436-R and PID2019-104863RB I00/AEI/10.13039/501100011033

Outline

- Solar disk observations
- Coronagraph observations
- CME reconstruction

- In situ observations
- ICME reconstruction
- Conciliation CME/ICME

- Conclusions

Financial support by the Spanish Ministerio de Ciencia, Innovación y Universidades FEDER/MCIU/AEI Projects ESP2017-88436-R and PID2019-104863RB I00/AEI/10.13039/501100011033

Outline

- Solar disk observations
- Coronagraph observations
- CME reconstruction

- In situ observations
- ICME reconstruction
- Conciliation CME/ICME

- Conclusions

Financial support by the Spanish Ministerio de Ciencia, Innovación y Universidades FEDER/MCIU/AEI Projects ESP2017-88436-R and PID2019-104863RB I00/AEI/10.13039/501100011033

Solar disk observations of the CME

Palmerio et al. 2017: "Determining the Intrinsic CME Flux Rope Type Using Remote-sensing Solar Disk Observations"

- ✓ Magnetic helicity sign: magnetic tongues, filament details, soft X-ray and/or extreme-ultraviolet sigmoids, skew of the coronal loops, flare ribbons, hemispheric helicity rule
- ✓ Axis orientation: tilt of the polarity inversion line, inclination of the post-eruption arcades
- ✓ Axial magnetic field direction: coronal dimmings to determine the flux rope footpoints and overlay the dimming regions onto line-of-sight magnetogram

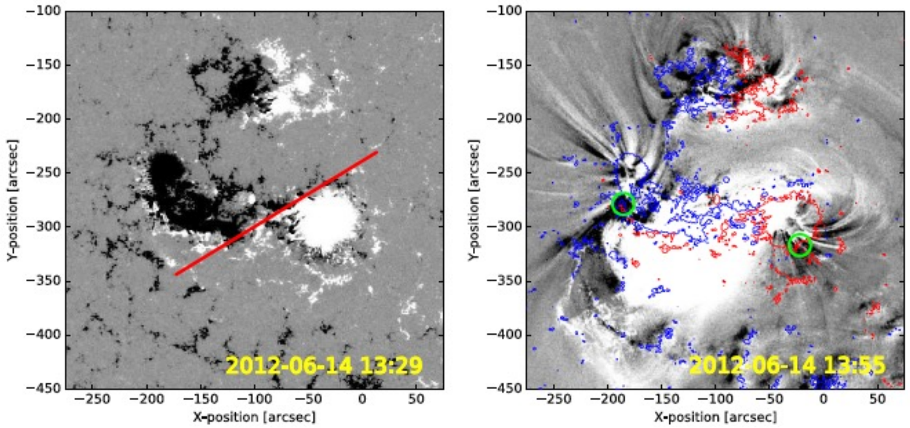

Palmerio et al. 2017

Magnetic Cloud Type	SEN	SWN	NES	NWS
Leading Field	South (-Bz)	South (-Bz)	North (+Bz)	North (+Bz)
Axial Field	East (+By)	West (-By)	East (+By)	West (-By)
Trailing Field	North (+Bz)	North (+Bz)	South (-Bz)	South (-Bz)
Helicity	LH	RH	RH	LH

NES-type

Kilpua et al. 2011

Financial support by the Spanish Ministerio de Ciencia, Innovación y Universidades FEDER/MCIU/AEI Projects ESP2017-88436-R and PID2019-104863RB I00/AEI/10.13039/501100011033

Solar disk observations of the CME

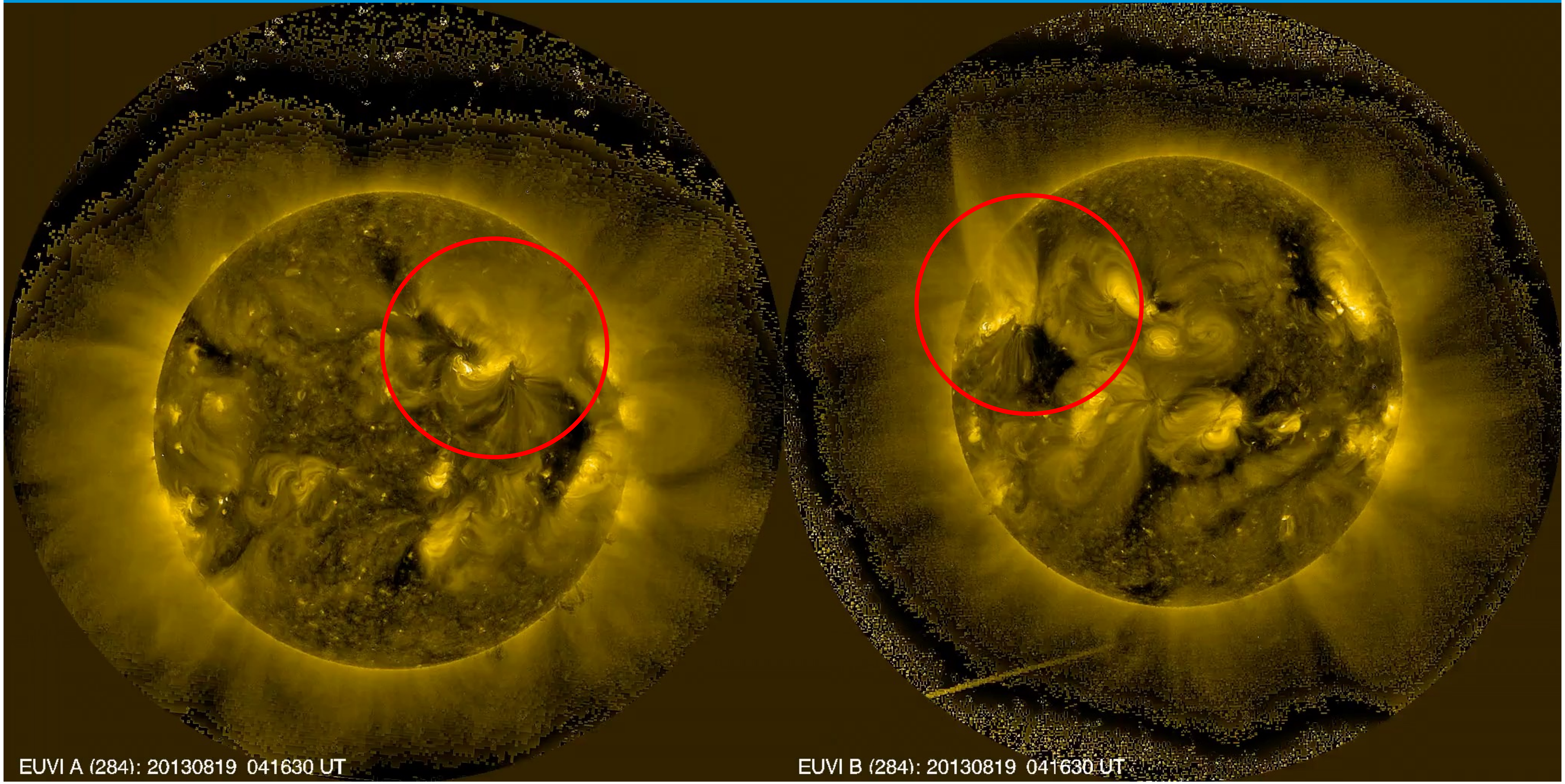

EUVI-A (left) and EUVI-B (right) 284Å channel images

Financial support by the Spanish Ministerio de Ciencia, Innovación y Universidades FEDER/MCIU/AEI Projects ESP2017-88436-R and PID2019-104863RB I00/AEI/10.13039/501100011033

Universidad de Alcalá
SPACE RESEARCH GROUP
SRG
MINISTERIO DE CIENCIA E INNOVACIÓN
UNIÓN EUROPEA
FONDO EUROPEO DE DESARROLLO REGIONAL
"Una manera de hacer Europa"
AGENCIA ESTATAL DE INVESTIGACIÓN

Solar disk observations of the CME

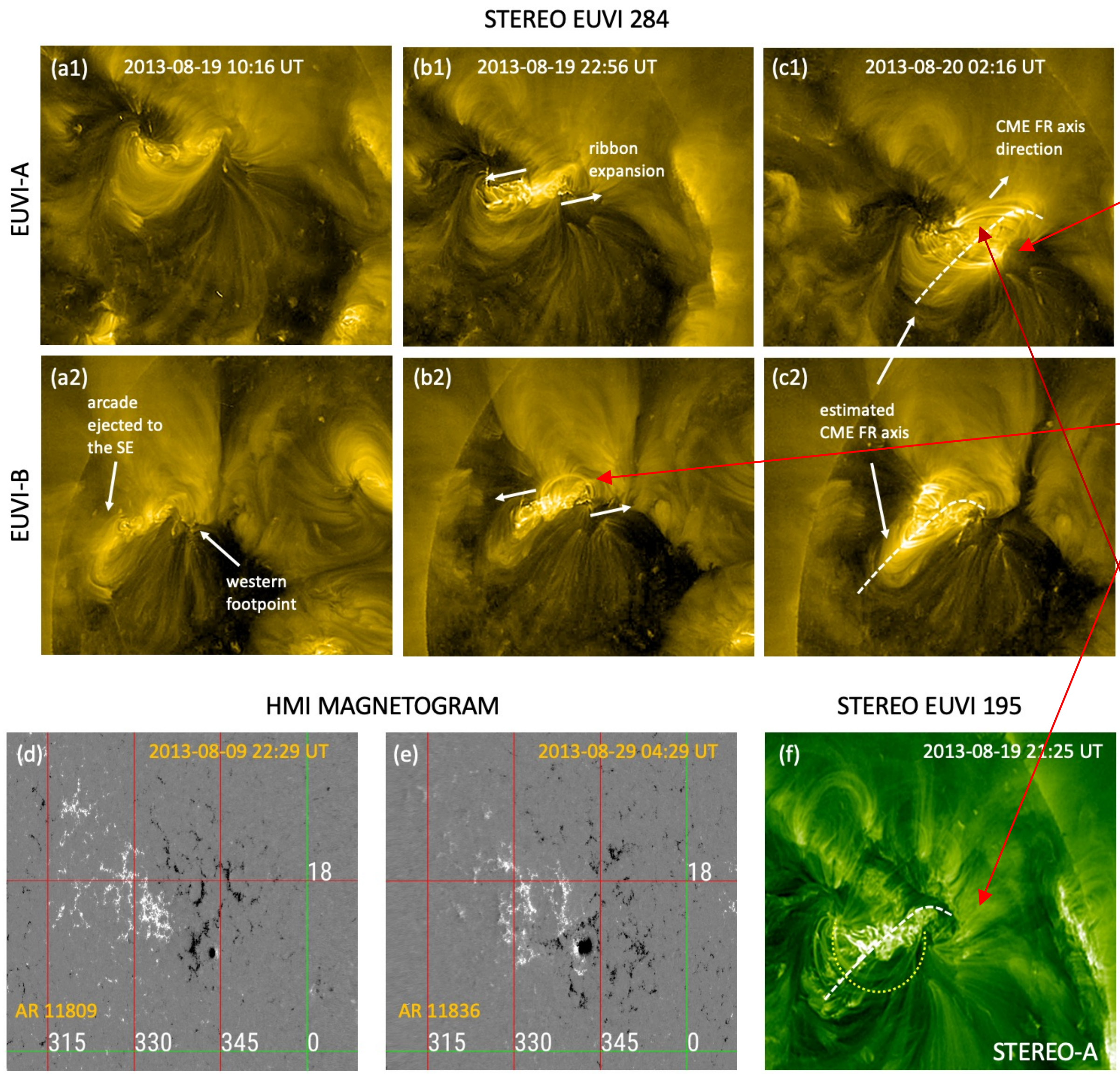

- Flux-rope tilt ~36°/22° (*PEAs orientation*)
- Positive chirality (*skew of the coronal loops:* right-skewed wrt PEAs as seen from positive polarity, *ribbon expansion*)
- Axial field direction to the west (*Bothmer & Schwenn 1994*: Field to the left as seen from positive polarity).

Palmerio et al. 2017

Financial support by the Spanish Ministerio de Ciencia, Innovación y Universidades FEDER/MCIU/AEI Projects ESP2017-88436-R and PID2019-104863RB I00/AEI/10.13039/501100011033

Solar disk observations of the CME

- Positive chirality
- Flux-rope tilt ~36°/22°
- Axial field direction to the west

Palmerio et al, 2017

"Curved axis"

Low-tilted cloud type South-West-North **(SWN)**

Kilpua et al, 2011

Magnetic Cloud Type	SEN	SWN	NES	NWS
Leading Field	South (-Bz)	South (-Bz)	North (+Bz)	North (+Bz)
Axial Field	East (+By)	West (-By)	East (+By)	West (-By)
Trailing Field	North (+Bz)	North (+Bz)	South (-Bz)	South (-Bz)
Helicity	LH	RH	RH	LH

Financial support by the Spanish Ministerio de Ciencia, Innovación y Universidades FEDER/MCIU/AEI Projects ESP2017-88436-R and PID2019-104863RB I00/AEI/10.13039/501100011033

Solar disk observations of the CME

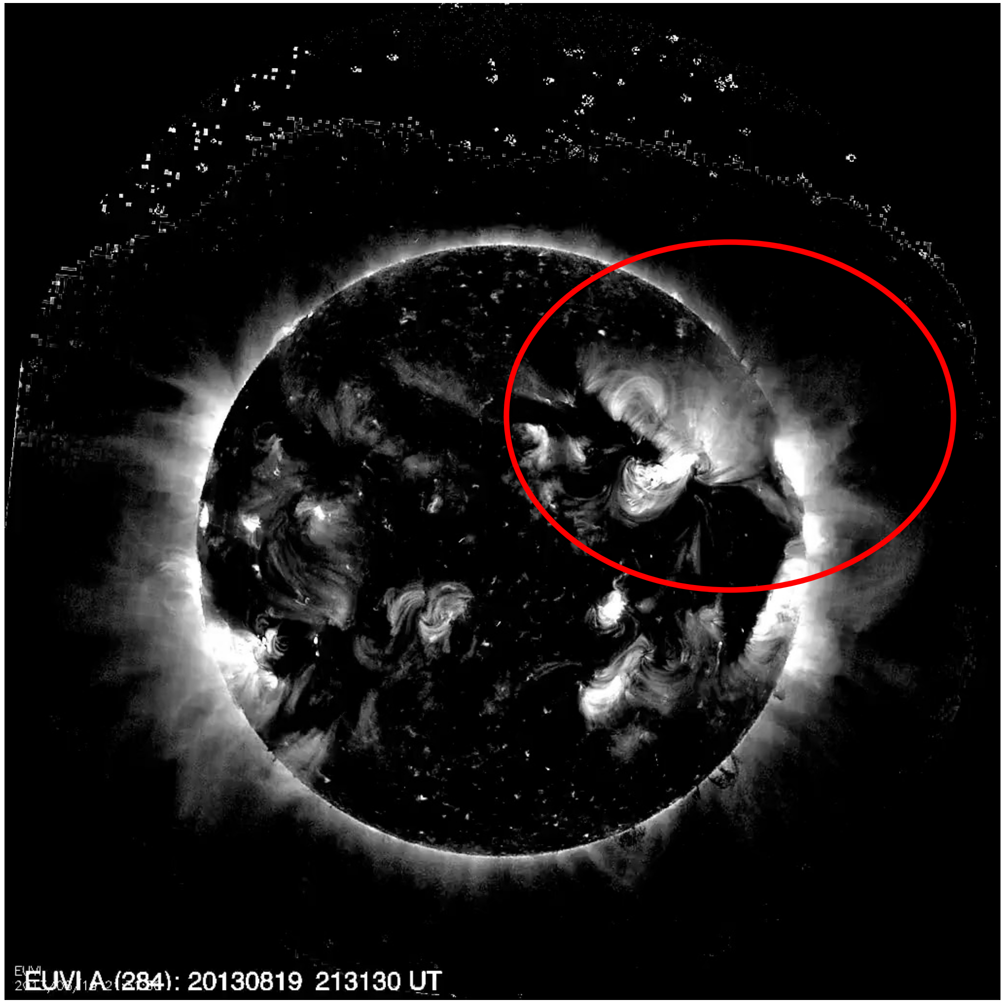

EUVI-A 284Å channel base-difference images
The base image was taken at 21:31 UT on August 19

Financial support by the Spanish Ministerio de Ciencia, Innovación y Universidades FEDER/MCIU/AEI Projects ESP2017-88436-R and PID2019-104863RB I00/AEI/10.13039/501100011033

Solar disk observations of the CME

EUVI-A 284Å channel base-difference images

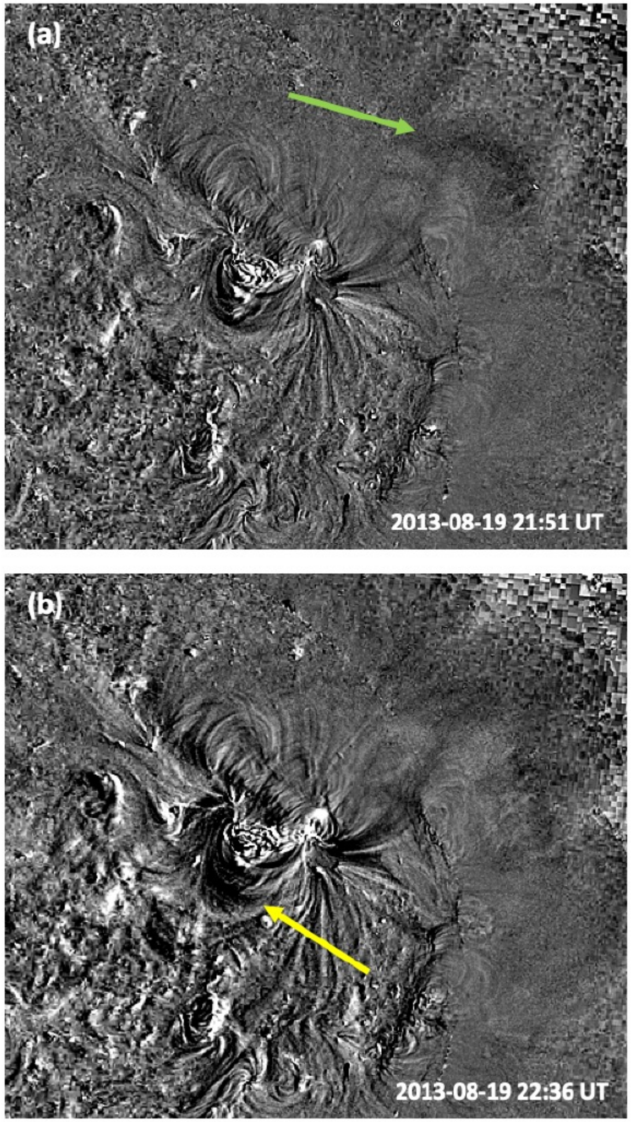

(a) Set of rising loops over the north-western area of the source AR becoming evident by 21:51 UT and marking the STEREO-B-directed part of the CME

Non-radial propagation (folding hand fun)

(b) Dimming along the south-eastern part of the AR by 22:36 UT marking the side of the eruption towards STEREO-A

Financial support by the Spanish Ministerio de Ciencia, Innovación y Universidades FEDER/MCIU/AEI Projects ESP2017-88436-R and PID2019-104863RB I00/AEI/10.13039/501100011033

Outline

- Solar disk observations
- Coronagraph observations
- CME reconstruction

- In situ observations
- ICME reconstruction
- Conciliation CME/ICME

- Conclusions

Financial support by the Spanish Ministerio de Ciencia, Innovación y Universidades FEDER/MCIU/AEI Projects ESP2017-88436-R and PID2019-104863RB I00/AEI/10.13039/501100011033

Coronagraph observations

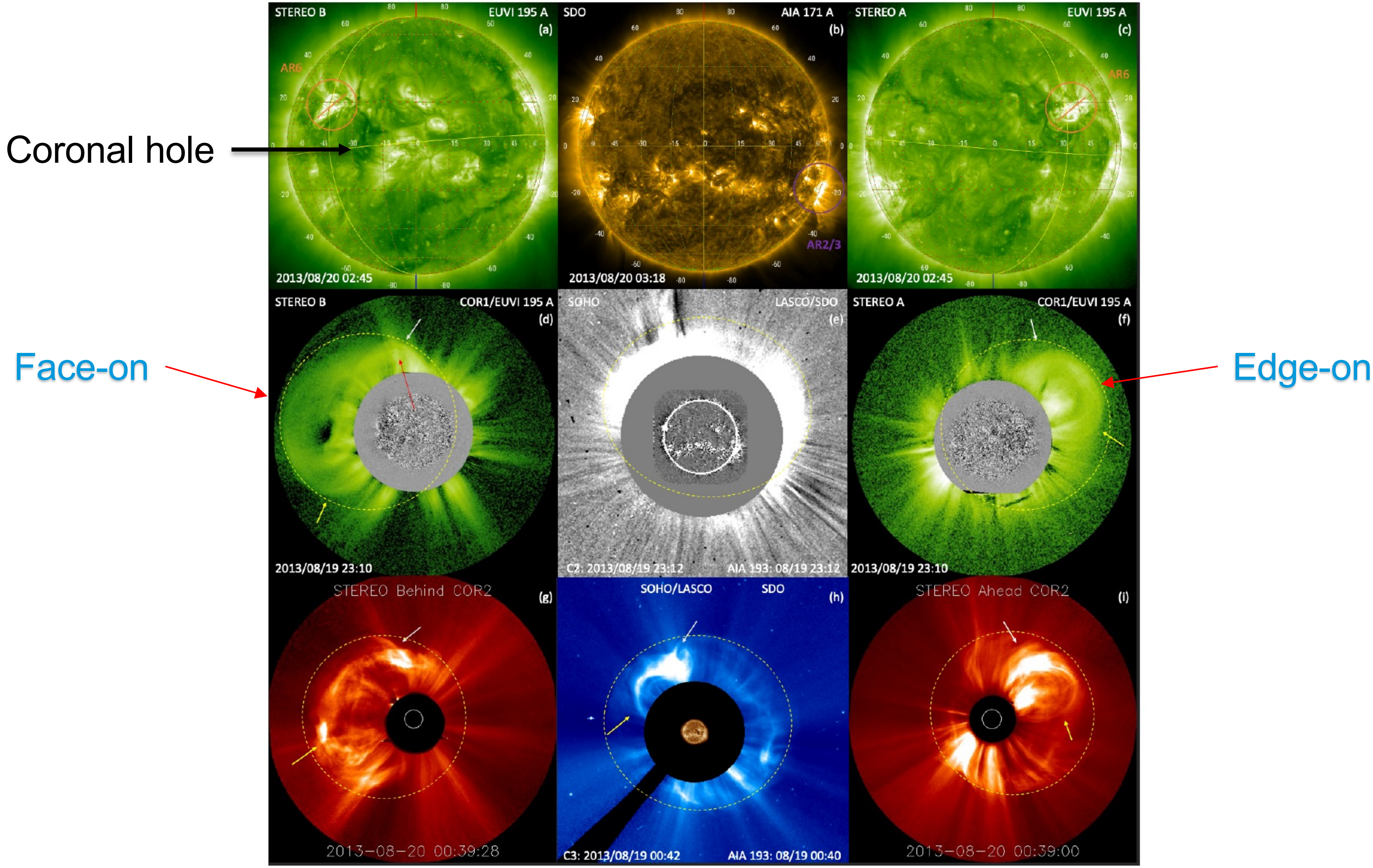

Financial support by the Spanish Ministerio de Ciencia, Innovación y Universidades FEDER/MCIU/AEI Projects ESP2017-88436-R and PID2019-104863RB I00/AEI/10.13039/501100011033

Coronagraph observations

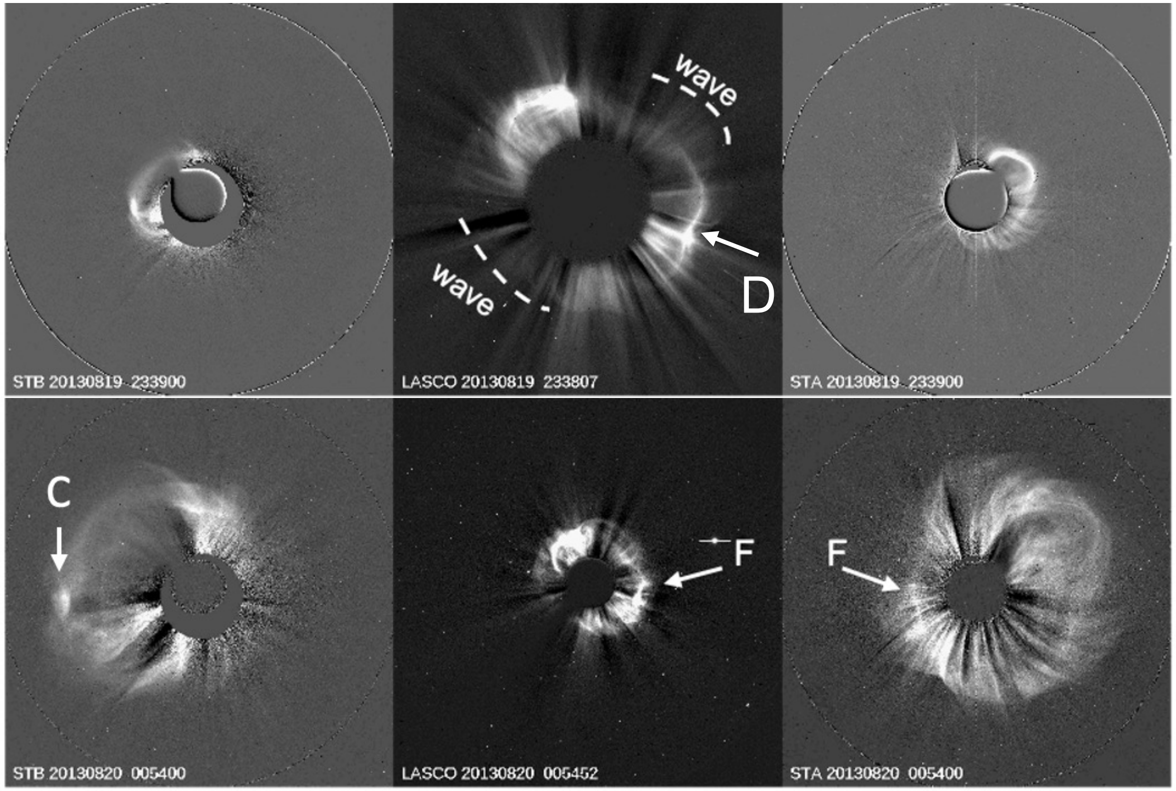

- C: compression towards MESSENGER and STEREO-A
- D: dimpled front (propagate along a streamer stalk)
- F: northern flank of the dimpled front
- C->F: Front strongly distorted along the position angle

Financial support by the Spanish Ministerio de Ciencia, Innovación y Universidades FEDER/MCIU/AEI Projects ESP2017-88436-R and PID2019-104863RB I00/AEI/10.13039/501100011033

Outline

- Solar disk observations
- Coronagraph observations
- CME reconstruction

- In situ observations
- ICME reconstruction
- Conciliation CME/ICME

- Conclusions

Financial support by the Spanish Ministerio de Ciencia, Innovación y Universidades FEDER/MCIU/AEI Projects ESP2017-88436-R and PID2019-104863RB I00/AEI/10.13039/501100011033

Graduated cylindrical shell (GCS) analysis

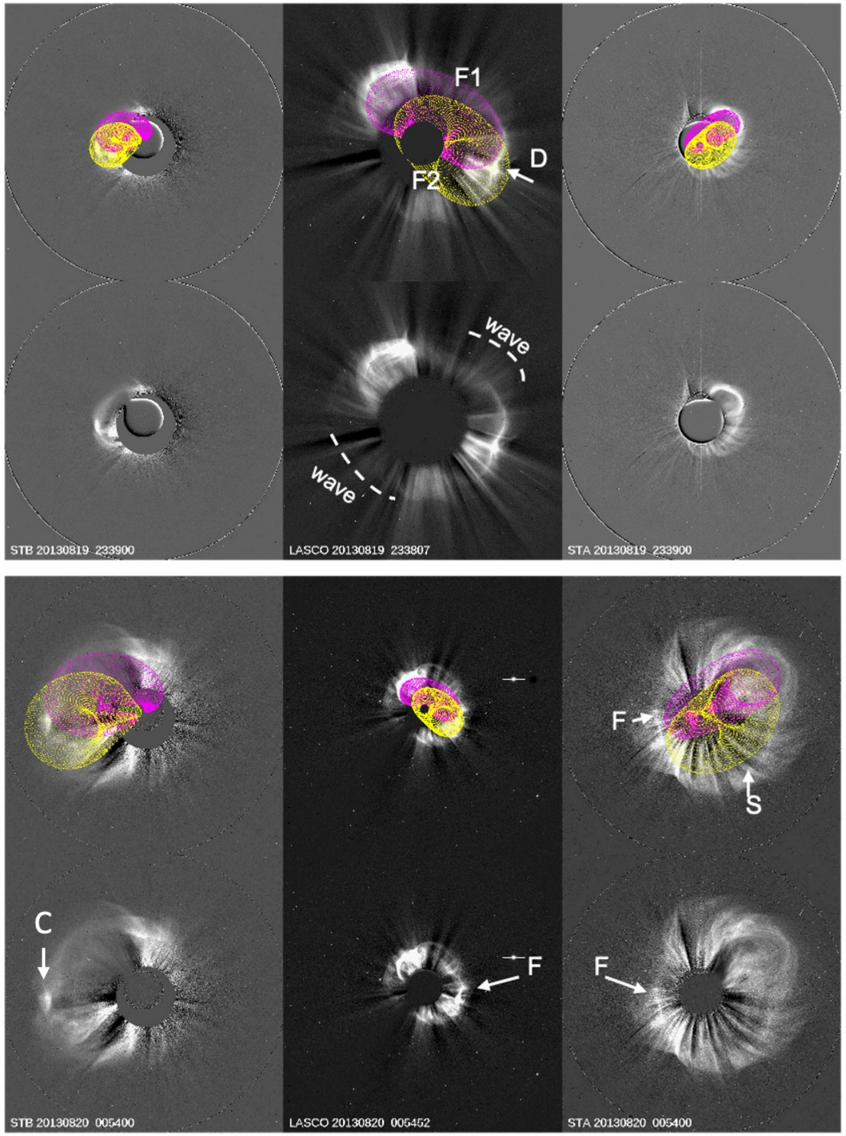

- Curved axis-> two GCS models
- 3D CME parameters is the convolution of both reconstructions (yellow and pink)

Good fitting (except D, S, F)

PyThea
Reconstruct the 3D structure of CMEs and shock waves

Financial support by the Spanish Ministerio de Ciencia, Innovación y Universidades FEDER/MCIU/AEI Projects ESP2017-88436-R and PID2019-104863RB I00/AEI/10.13039/501100011033

Graduated cylindrical shell (GCS) analysis

Table 2. Three-dimensional CME properties derived from the GCS fits shown in Fig. 6.

Date-Time (UT in 2013)	Lon (deg)		Lat (deg)		Tilt (deg)		Height ($R_\odot$)		Half-angle (–)		Ratio (deg)		R_{maj} (deg)		R_{min} (deg)	
	F1	F2	F1	F2	F1	F2	F1	F2	F1	F2	F1	F2	F1	F2	F1	F2
(1)	(2)	(3)	(4)	(5)	(6)	(7)	(8)	(9)	(10)	(11)	(12)	(13)	(14)	(15)	(16)	(17)
08-19 23:24	172	160	13	−10	22	36	5.2	5.0	50	25	0.35	0.40	70	49	20	24
08-19 23:39	171	160	13	−10	22	36	6.3	6.9	52	25	0.35	0.40	72	49	20	24
08-19 23:54	171	160	13	−10	22	36	7.1	8.2	65	25	0.35	0.40	85	49	20	24
08-20 00:24	171	160	13	−10	22	36	9.8	11.1	65	25	0.35	0.40	85	49	20	24
08-20 00:39	170	160	13	−10	22	36	11.4	13.2	65	25	0.35	0.40	85	49	20	24
08-20 00:54	170	160	13	−10	22	36	12.6	14.7	65	25	0.35	0.40	85	49	20	24

Notes. Column (1): date and time UT in 2013. Columns (2)–(5): Stonyhurst coordinates of the F1 and F2 leading-edge (LE) orientation. Columns (6)–(13): F1 and F2 angle with respect to the solar equator, height from the Sun centre, half-angle, and aspect ratio. Columns (14)–(17): F1 and F2 face-on half-width (R_{min} + half-angle) and edge-on half-width (arcsin(ratio)) according to Thernisien (2011).

Self-similar expansion

Financial support by the Spanish Ministerio de Ciencia, Innovación y Universidades FEDER/MCIU/AEI Projects ESP2017-88436-R and PID2019-104863RB I00/AEI/10.13039/501100011033

Graduated cylindrical shell (GCS) analysis

- Flux-rope tilt ~36° (east)/ 22° (west)
- CME width: 119°, expected being observed at STEREO-B (lower part of the west flank of F1)

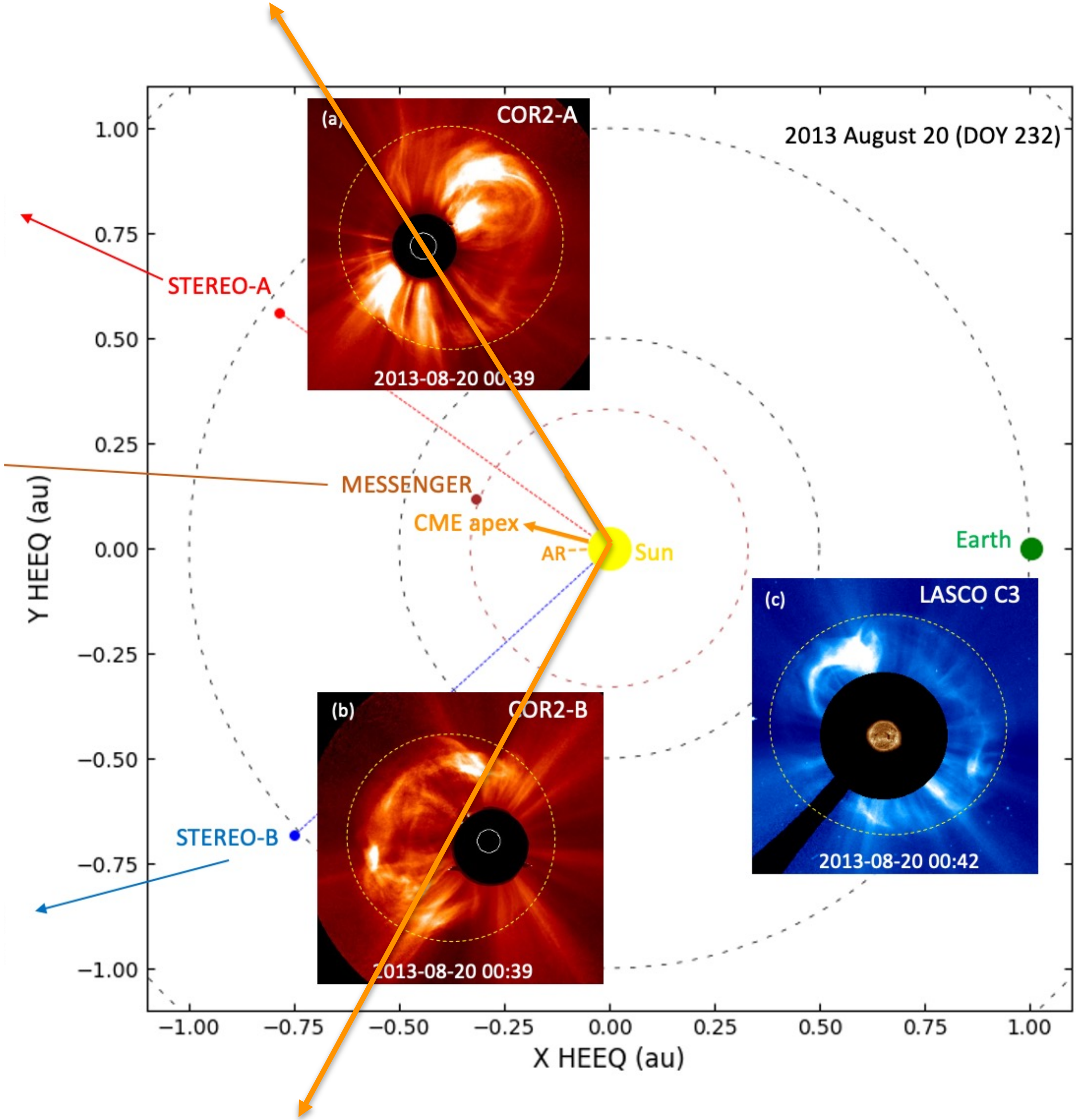

Financial support by the Spanish Ministerio de Ciencia, Innovación y Universidades FEDER/MCIU/AEI Projects ESP2017-88436-R and PID2019-104863RB I00/AEI/10.13039/501100011033

Outline

- ❖ Solar disk observations
- ❖ Coronagraph observations
- ❖ CME reconstruction

- ❖ In situ observations
- ❖ ICME reconstruction
- ❖ Conciliation CME/ICME

- ❖ Conclusions

Financial support by the Spanish Ministerio de Ciencia, Innovación y Universidades FEDER/MCIU/AEI Projects ESP2017-88436-R and PID2019-104863RB I00/AEI/10.13039/501100011033

In situ observations

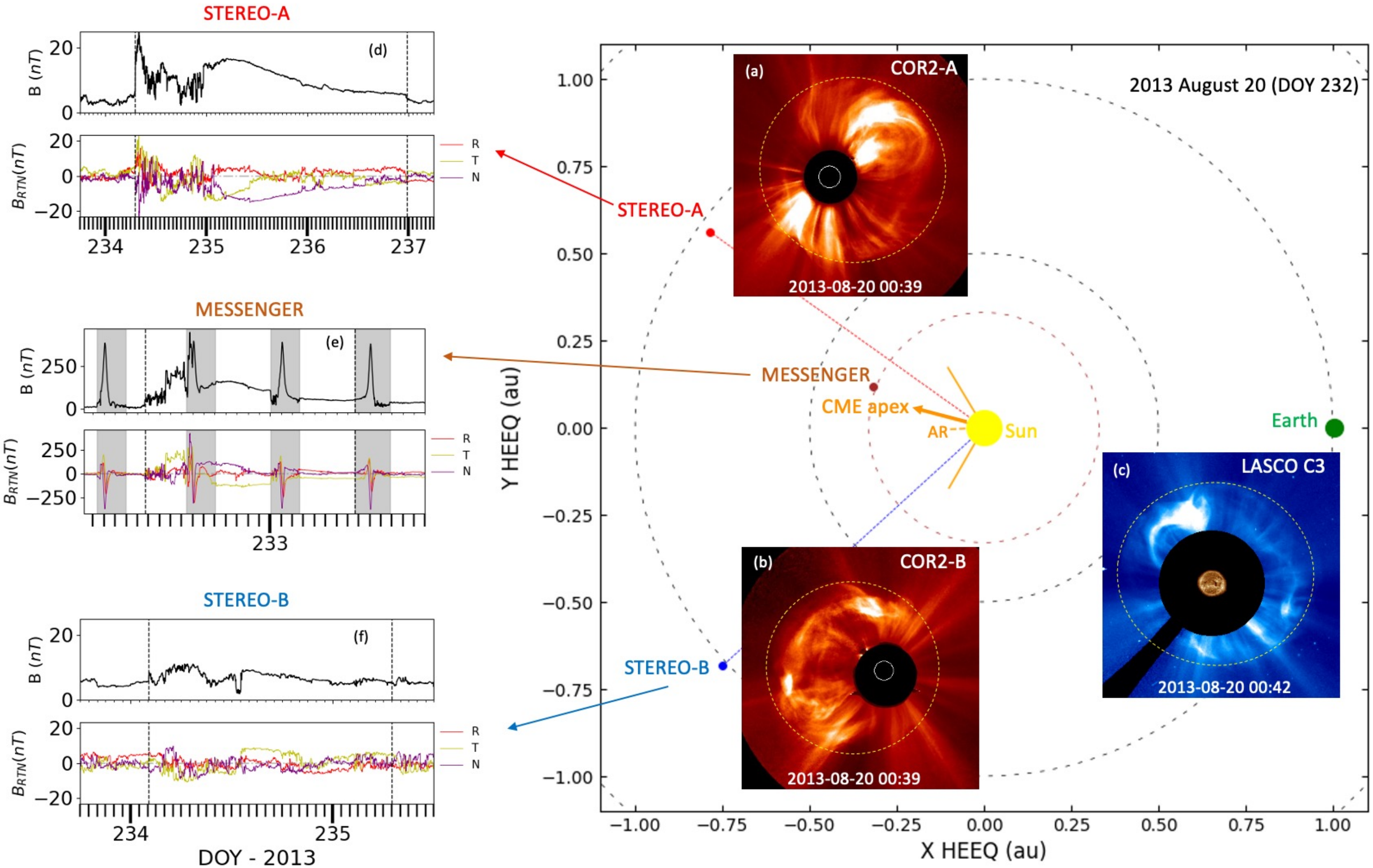

Financial support by the Spanish Ministerio de Ciencia, Innovación y Universidades FEDER/MCIU/AEI Projects ESP2017-88436-R and PID2019-104863RB I00/AEI/10.13039/501100011033

In situ observations

Table 3. ICME signatures observed at different spacecraft.

s/c	ICME T_{start}	ICME T_{end}	MO T_{start}	MO T_{end}	MC T_{start}	MC T_{end}	MC-like T_{start}	MC-like T_{end}	V_{sw} ICME (km s^{-1})	B_{max} (nT)	B'_{max} MO (nT)	V_{sw} MO (km s^{-1})	FR type
	(DOY in 2013)												
(1)	(2)	(3)	(4)	(5)	(6)	(7)	(8)	(9)	(10)	(11)	(12)	(13)	(14)
MESS	232.53	233.32	232.79	233.32	232.79	233.00	233.11	233.32	800[a]	168.9	28.8	575[a]	NES
STB	234.09	235.29	234.54	234.89	234.54	234.75	–	–	600	9.2	10.0	568	WSE
STA	234.29	236.98	234.97	236.98	235.02	236.05	236.17	236.98	455	16.6	16.6	398	ESW

Notes. Column 1: observing spacecraft. Columns 2–9: start and end of the ICME, MO, MC, and MC-like structures, respectively. Column 10: mean solar wind speed within the ICME. Columns 11–13: maximum magnetic field strength, scaled magnetic field strength to the heliocentric distance of STEREO-A (details given in the main text), and mean solar wind speed within the MO, respectively. Column 14: type of field rotation (e.g. Bothmer & Schwenn 1998) determined by eye. [a] MESSENGER mean speed taken from the ENLIL simulation (Sect. 5.2 in Paper I).

- *Half longitudinal extension* of the CME: distance between MESS and STB: Average width of the ICME: 110º, much larger than statistical studies (Yashiro et al. 2004)
- *Radial diameter* for the ICME, MO, MC (Kilpua et al. 2011) at different locations (Gosling 1990, Leitner et al. 2007): MESSENGER and STEREO-A are observing similar MC structure
- *Aspect ratio*: similar at MESSENGER and STEREO-A
- *Average speed of expansion*: Above the mean value (Nieves-Chinchilla et al. 2018b)
- *Maximum magnetic field* (Leitner et al. 2007): MESSENGER is located close to the nose of the ICME and STEREO-B closer to the flank than STERO-A.
- *Magnetic field configuration* (NES, WSE, ESW)
- *Distortion parameter (DiP)* (Nieves-Chinchilla et al. 2018b)
- *Total pressure:* closest approach of a spacecraft from the core of the ICME (Russel et al. 2005)

Financial support by the Spanish Ministerio de Ciencia, Innovación y Universidades FEDER/MCIU/AEI Projects ESP2017-88436-R and PID2019-104863RB I00/AEI/10.13039/501100011033

In situ observations

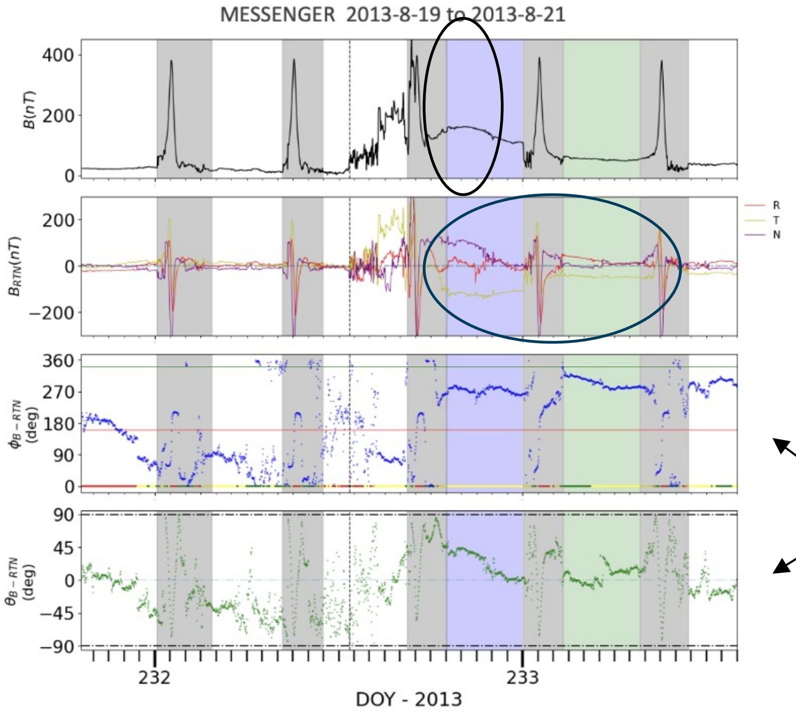

MESSENGER (0.33 au)

(No plasma info)

- Compression at the front

  DiP parameter=0.44 (distortion or expansion?)

- Complex structure:
  - -MC in blue (Burlaga et al. 1981)
  - -MC-like in green

- NES (low tilted) ⟶ Positive helicity

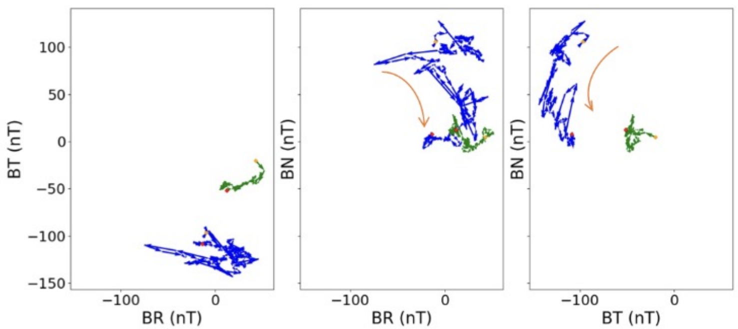

Magnetic Cloud Type	SEN	SWN	NES	NWS
Leading Field	South (-Bz)	South (-Bz)	North (+Bz)	North (+Bz)
Axial Field	East (+By)	West (-By)	East (+By)	West (-By)
Trailing Field	North (+Bz)	North (+Bz)	South (-Bz)	South (-Bz)
Helicity	LH	RH	RH	LH

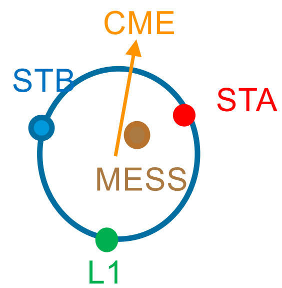

Financial support by the Spanish Ministerio de Ciencia, Innovación y Universidades FEDER/MCIU/AEI Projects ESP2017-88436-R and PID2019-104863RB I00/AEI/10.13039/501100011033

In situ observations

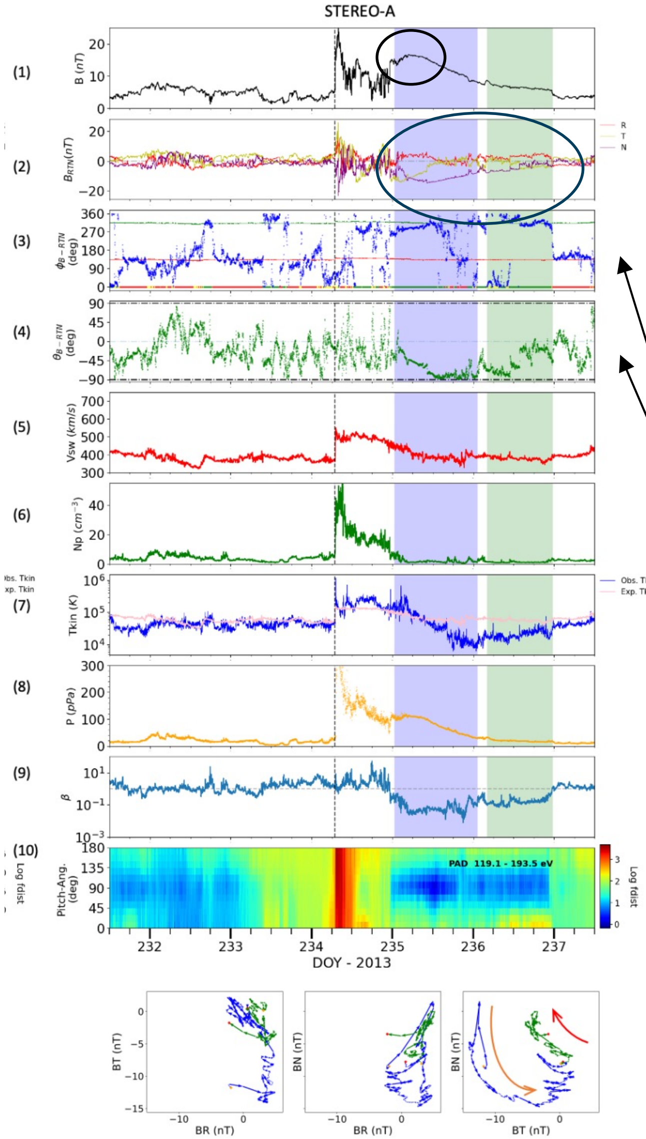

STEREO-A (0.97 au)

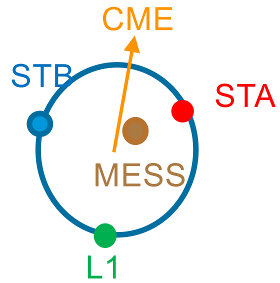

- Higher compression at the front (DiP parameter=0.42; V_{exp}=33.5 km/s)
- Complex structure:
  - -MC in blue (Burlaga et al. 1981)
  - -MC-like in green
- ESW (high tilted) → Positive helicity

Magnetic Cloud Type	WNE	ESW	ENW	WSE
Leading Field	West (-By)	East (+By)	East (+By)	West (-By)
Axial Field	North (+Bz)	South (-Bz)	North (+Bz)	South (-Bz)
Trailing Field	East (+By)	West (-By)	West (-By)	East (+By)
Helicity	RH	RH	LH	LH

Financial support by the Spanish Ministerio de Ciencia, Innovación y Universidades FEDER/MCIU/AEI Projects ESP2017-88436-R and PID2019-104863RB I00/AEI/10.13039/501100011033

In situ observations

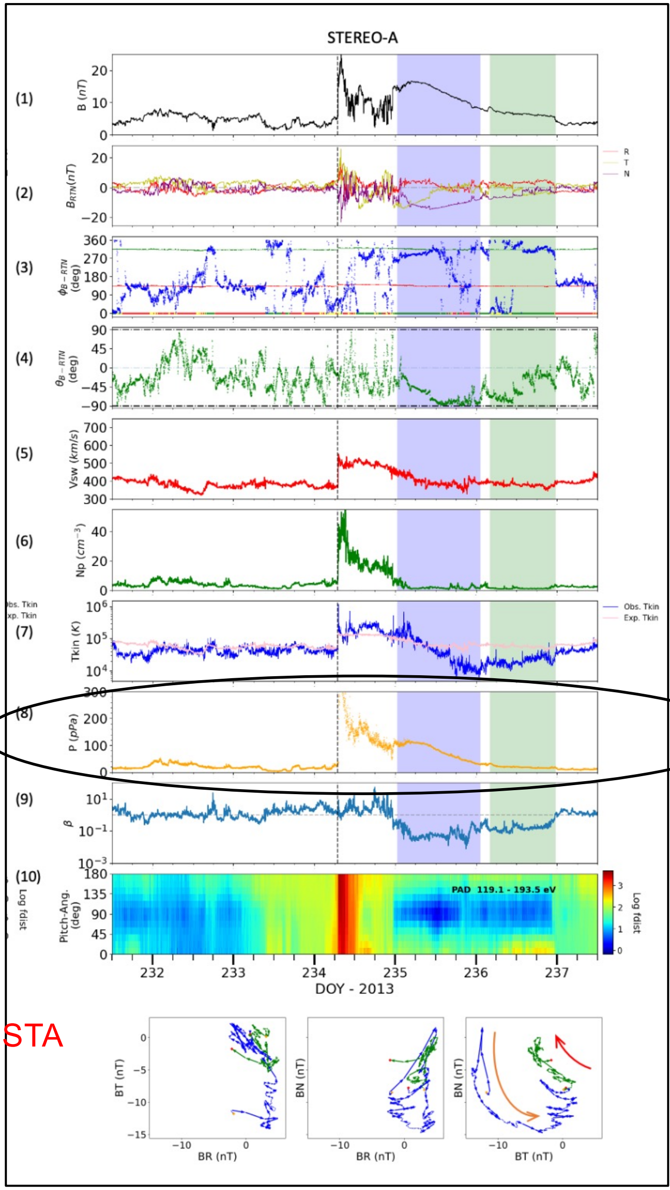

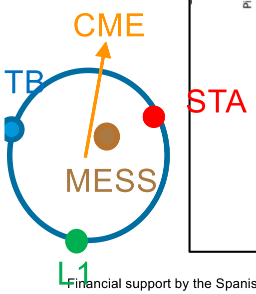

STEREO-A (0.97 au) cont.

- *Total pressure* (Russel et al. 2005): prompt and large increase followed by a half-day plateau and then a gradual decay

Close to core encounter
Group 2 ICMEs (Jian et al. 2006)

- Total pressure and magnetic field are stronger at STEREO-A than at STEREO-B

Financial support by the Spanish Ministerio de Ciencia, Innovación y Universidades FEDER/MCIU/AEI Projects ESP2017-88436-R and PID2019-104863RB I00/AEI/10.13039/501100011033

In situ observations

STEREO-B (1.02 au)

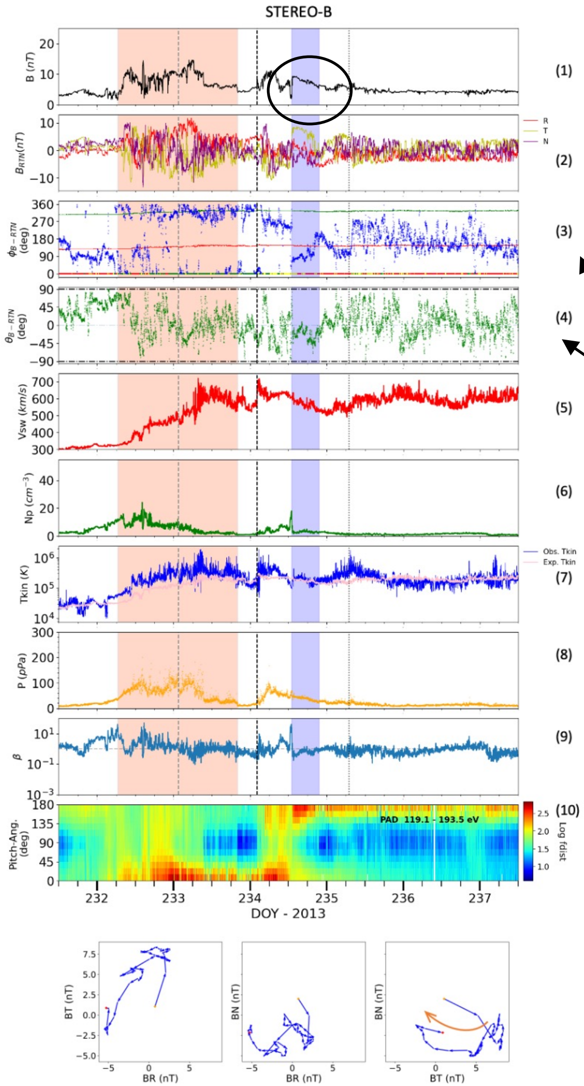

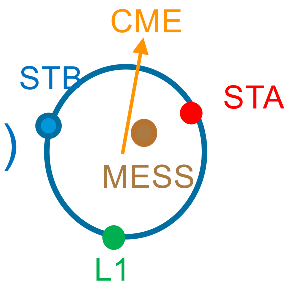

- MC (blue shaded area, Burlaga et al. 1981)
- DiP=0.48 (symmetric profile); V_{exp}=33.5 km/s
- WSE (high tilted) → Negative helicity

Magnetic Cloud Type	WNE	ESW	ENW	WSE
Leading Field	West (-By)	East (+By)	East (+By)	West (-By)
Axial Field	North (+Bz)	South (-Bz)	North (+Bz)	South (-Bz)
Trailing Field	East (+By)	West (-By)	West (-By)	East (+By)
Helicity	RH	RH	LH	LH

Financial support by the Spanish Ministerio de Ciencia, Innovación y Universidades FEDER/MCIU/AEI Projects ESP2017-88436-R and PID2019-104863RB I00/AEI/10.13039/501100011033

In situ observations

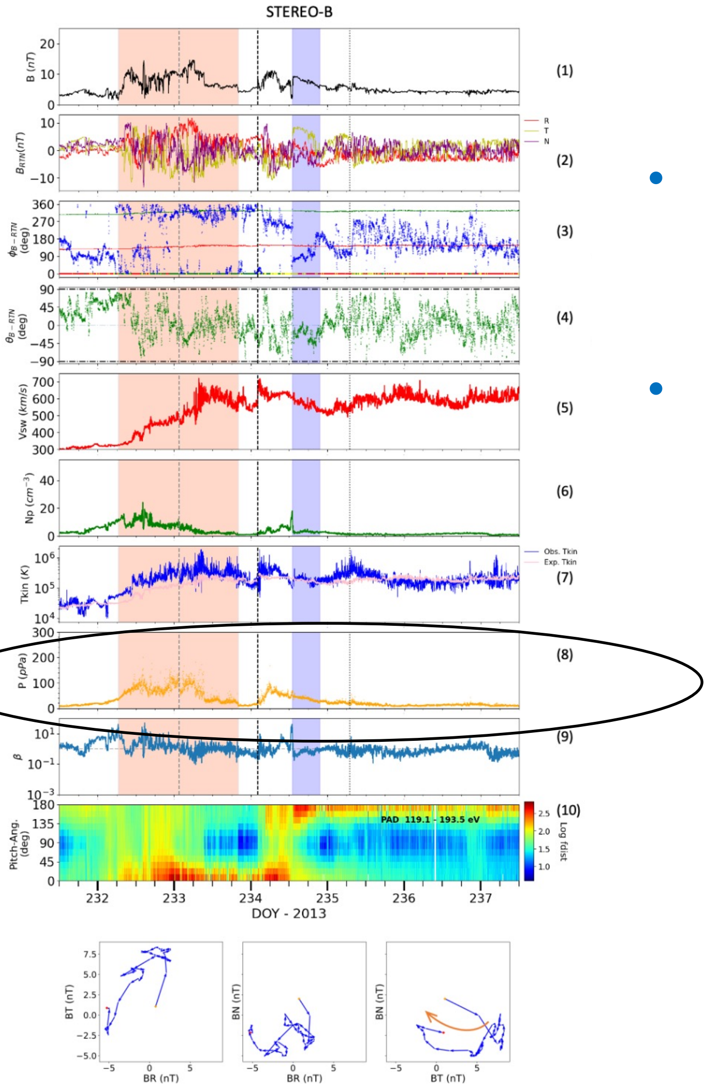

STEREO-B (1.02 au) cont.

- *ICME arrives earlier at STEREO-B (coronal hole)*
- *Total pressure* (Russel et al. 2005): gradual increase, followed by a gradual decay

ICME is crossed far from the centre
Group 3 ICMEs (Jian et al. 2006)

Financial support by the Spanish Ministerio de Ciencia, Innovación y Universidades FEDER/MCIU/AEI Projects ESP2017-88436-R and PID2019-104863RB I00/AEI/10.13039/501100011033

Outline

- Solar disk observations
- Coronagraph observations
- CME reconstruction

- In situ observations
- ICME reconstruction
- Conciliation CME/ICME

- Conclusions

Financial support by the Spanish Ministerio de Ciencia, Innovación y Universidades FEDER/MCIU/AEI Projects ESP2017-88436-R and PID2019-104863RB I00/AEI/10.13039/501100011033

In situ analysis
Elliptical Cylindrical (EC)-model

Table 3. EC model fit parameters in RTN coordinates.

s/c	Longitude ϕ (deg)	Tilt θ (deg)	Rotation ξ (deg)	Ellipse ratio δ (-)	Cross-section Radius R (au)	Distance Y_0 (au)	χ^2	Chirality
(1)	(2)	(3)	(4)	(5)	(6)	(7)	(8)	(9)
MESSENGER MC	115	25	73	0.44	0.052	-0.019	0.15	Positive
STEREO-B MC	238	-13	134	0.68	0.137	0.109	0.29	Negative
STEREO-A MC	145	-46	79	0.67	0.160	-0.086	0.22	Positive

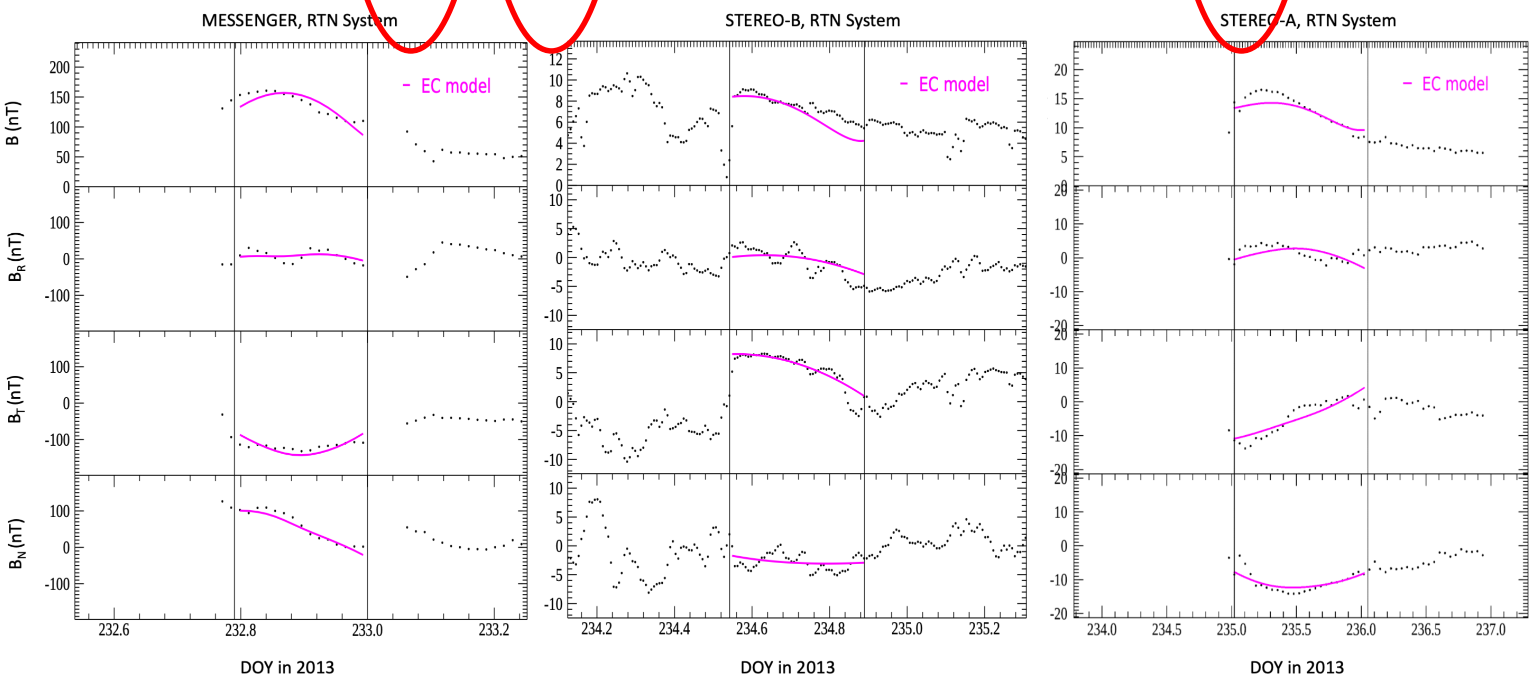

Financial support by the Spanish Ministerio de Ciencia, Innovación y Universidades FEDER/MCIU/AEI Projects ESP2017-88436-R and PID2019-104863RB I00/AEI/10.13039/501100011033

Outline

- Solar disk observations
- Coronagraph observations
- CME reconstruction

- In situ observations
- ICME reconstruction
- **Conciliation CME/ICME**

- Conclusions

Financial support by the Spanish Ministerio de Ciencia, Innovación y Universidades FEDER/MCIU/AEI Projects ESP2017-88436-R and PID2019-104863RB I00/AEI/10.13039/501100011033

Remote-sensing/In-situ reconciliation

Remote observations	In situ observations
✓ Distortion (compression) at C	✓ DiP parameter STEREO-A
✓ Non radial (widespread) propagation	✓ Observed at both STEREO
✓ Coronal hole near STEREO-B location	✓ Earlier arrival to STEREO-B
✓ Relative position between CME nose and s/c position given by GCS model	✓ Impact parameter in the EC-model ✓ Longitude/Latitude in EC-model ✓ Total pressure measured
✓ Flux-rope type	x MC type
✓ Flux-rope Helicity	x MC helicity

Financial support by the Spanish Ministerio de Ciencia, Innovación y Universidades FEDER/MCIU/AEI Projects ESP2017-88436-R and PID2019-104863RB I00/AEI/10.13039/501100011033

Remote-sensing/In-situ reconciliation

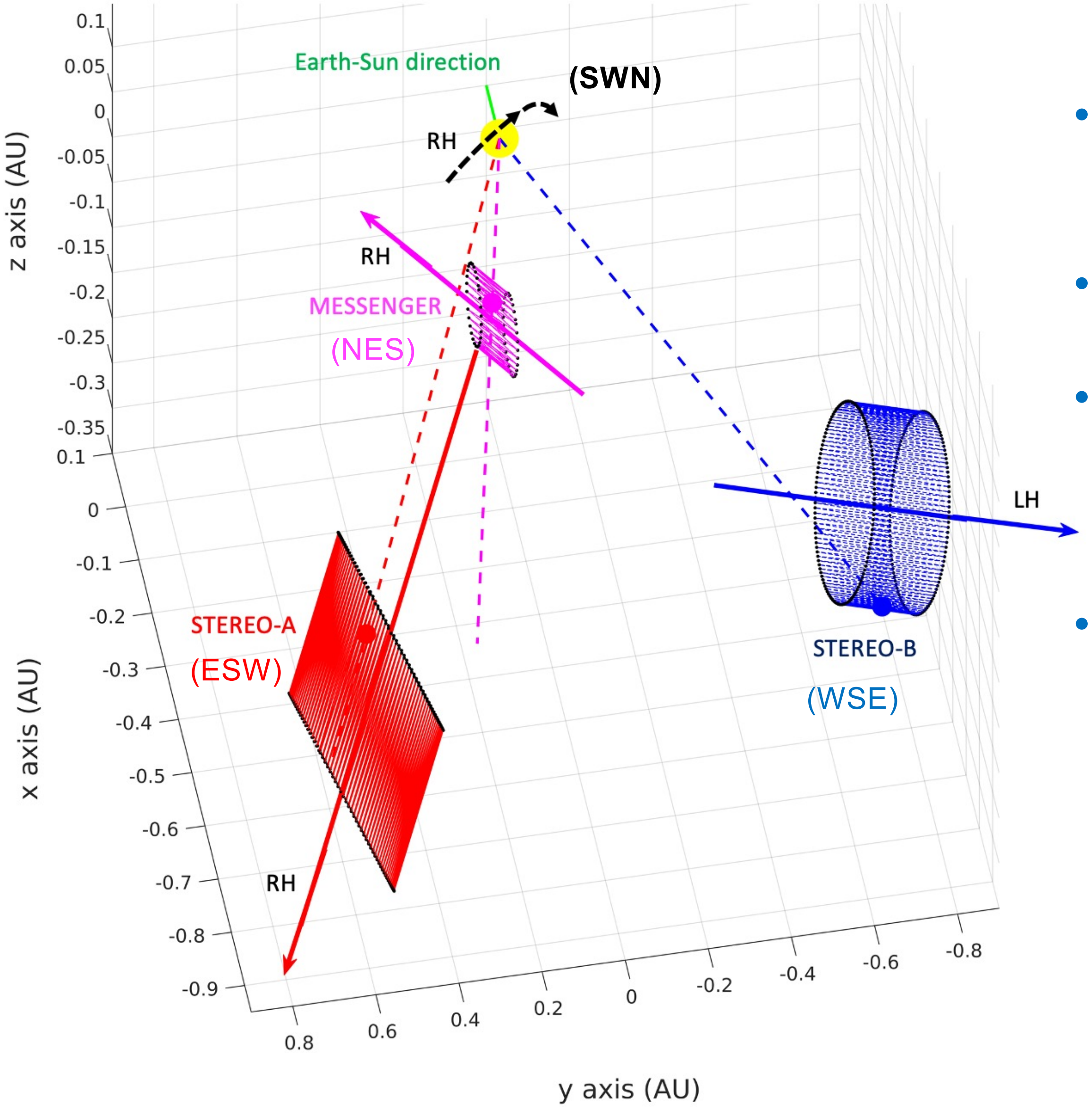

- Positive helicity at MESSENGER and STEREO-A
- Negative helicity at STEREO-B
- STEREO-B cylinder: similar orientation of the west side of the MFR
- MESSENGER and STEREO-A cylinders: different orientations from the east side of the MFR

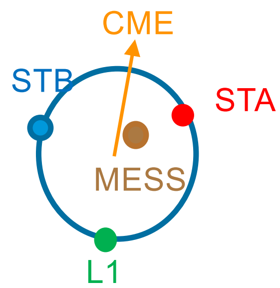

Financial support by the Spanish Ministerio de Ciencia, Innovación y Universidades FEDER/MCIU/AEI Projects ESP2017-88436-R and PID2019-104863RB I00/AEI/10.13039/501100011033

Outline

- Solar disk observations
- Coronagraph observations
- CME reconstruction

- In situ observations
- ICME reconstruction
- Conciliation CME/ICME

- **Conclusions**

Financial support by the Spanish Ministerio de Ciencia, Innovación y Universidades FEDER/MCIU/AEI Projects ESP2017-88436-R and PID2019-104863RB I00/AEI/10.13039/501100011033

Conclusions

#1 **Wide, curved, highly distorted, and rather complex CME** showed different orientations as observed on the solar disk and measured in situ at 0.3 au and near 1 au.

#2 **Ambient conditions can significantly affect the expansion and propagation** of the CME and ICME, introducing additional irregularities to the already asymmetric eruption (coronal hole, heliospheric plasma sheet)

#3 These complex structures **cannot be directly reconstructed** with the currently available models (two GCS fits, EC-model with distortion)

#4 **Multi-point analysis** is of the utmost importance in such complex events.

l.rodriguezgarcia@uah.es

Financial support by the Spanish Ministerio de Ciencia, Innovación y Universidades FEDER/MCIU/AEI Projects ESP2017-88436-R and PID2019-104863RB I00/AEI/10.13039/501100011033